Mechanically Pattern Reconfigurable Yagi–Uda Monopole Antenna Using Magnetic Gear

Keisuke Konno, *Senior Member, IEEE*, Satoshi Yoshida, *Member, IEEE*, Sho Muroga, *Member, IEEE*, Nozomi Haga, *Member, IEEE*, Jerdvisanop Chakarothai, *Senior Member, IEEE*, Qiang Chen, *Senior Member, IEEE*, and Gabriele Gradoni, *Member, IEEE*

***Abstract*—In this article, a novel mechanically reconfigurable Yagi–Uda monopole antenna using a magnetic gear is proposed. The proposed antenna is composed of a folded monopole element and floating inverse T-shaped director/reflector elements. As the floating inverse T-shaped director/reflector elements rotate, the main beam direction of the proposed antenna scans. A magnetic gear is introduced to rotate the floating inverse T-shaped director/reflector elements in a mechanically contactless manner. Due to the magnetic gear, the proposed antenna is free from a mechanical connection between antenna elements and actuators. A prototype of the proposed antenna is designed at the 2.5 GHz-band and is fabricated, including a mechanical control system for the magnetic gear. Finally, radiation performance and reconfigurability of the proposed antenna are clarified numerically and experimentally.**

***Index Terms*—Direct-drive system, magnetic gear, reconfigurable antenna, Yagi–Uda antenna.**

I. Introduction

RECONFIGURABLE antennas are promising candidates for the next generation wireless systems because their directivity, operating frequency, and other functionalities are tunable. The reconfigurable antennas are roughly categorized into electronic ones and mechanical ones.

Extensive efforts have been dedicated to developing electronically reconfigurable antennas. Most of the electronically reconfigurable antennas use a diode as a reactance, and their radiation performance is tunable by applying bias voltage to the diode. The concept of reactively controlled array antennas has been proposed by Harrington [1] and experimentally demonstrated by Dinger [2]. One of the popular reactively controlled array antennas is the electronically steerable parasitic array radiator (ESPAR) antenna [3], [4], [5], [6], [7], [8], [9]. The ESPAR antenna is composed of a driven element surrounded by parasitic elements with varactor diodes, and its beam direction is switchable by applying bias voltage to the diodes. Although the original ESPAR antenna is composed of monopole elements, various ESPAR antennas composed of patch or slot elements have been developed in [10], [11], [12], and [13]. Frequency reconfigurable quasi-Yagi dipole antenna using the varactor diodes has been developed at the 2-GHz band and extended to base station or cognitive radio applications [14], [15], [16]. Beam switching or pattern reconfigurable Yagi–Uda antennas have been developed so far [17], [18], [19]. Although high-speed tunability is a big advantage of the electronically reconfigurable antennas, insertion loss and nonlinearity of the diodes are major disadvantages.

As counterparts of the electronically reconfigurable antennas, mechanically reconfigurable antennas have been developed. The mechanically reconfigurable antennas actuate the shape, position, or angle of an antenna. For example, deformation of a reflector or subreflector surface using actuators has been introduced to design reconfigurable reflector antennas [20], [21], [22], [23]. Mechanically reconfigurable reflectarrays using motors or actuators have been proposed, and their angle/height tunability has been demonstrated [24], [25], [26]. A mechanically pattern reconfigurable dipole array antenna on a two-wire parallel line has been proposed, and its beam scanning capability has been clarified [27], [28]. In recent years, a radial line planar phased array antenna using rotatable helical antenna elements by micromotors has been proposed [29]. Although the mechanically reconfigurable antennas are free from insertion loss and nonlinearity of the diodes, the complicated mechanical connection between antenna elements and actuators is a disadvantage during fabrication. Also, the friction and abrasion of mechanical gears are disadvantages. To overcome these disadvantages, reconfigurable reflectarray antennas using electromagnets have been proposed in [30], [31], and [32]. Owing to the electromagnets, the height of reflectarray elements is tunable in a contactless manner, and a complicated mechanical connection between antenna elements

Received 14 August 2025; revised 12 January 2026; accepted 22 January 2026. Date of publication 12 February 2026; date of current version 11 May 2026. This work was supported in part by the Japan Society for the Promotion of Science (JSPS) KAKENHI under Grant 22K04061 and in part by the Tohoku University Young Leaders Overseas Program. *(Corresponding author: Keisuke Konno.)*

Keisuke Konno and Qiang Chen are with the Department of Communications Engineering, Graduate School of Engineering, Tohoku University, Sendai 980-8579, Japan (e-mail: keisuke.konno.b5@tohoku.ac.jp; qiang.chen.a5@tohoku.ac.jp).

Satoshi Yoshida is with the Course of Electronics, Information and Communication Engineering, Faculty of Advanced Science and Technology, Ryukoku University, Otsu 520-2194, Japan (e-mail: yoshida123@rins.ryukoku.ac.jp).

Sho Muroga is with the Department of Electrical Engineering, Graduate School of Engineering, Tohoku University, Sendai 980-8579, Japan (e-mail: sho.muroga.e1@tohoku.ac.jp).

Nozomi Haga is with the Department of Electrical and Electronic Information Engineering, Toyohashi University of Technology, Toyohashi 441-8580, Japan (e-mail: haga.nozomi.ok@tut.jp).

Jerdvisanop Chakarothai is with the National Institute of Information and Communications Technology, Koganei 184-8795, Japan (e-mail: jerd@nict.go.jp).

Gabriele Gradoni is with the 6G Innovation Center, Institute for Communication Systems, University of Surrey, GU2 7XH Guildford, U.K., and also with the Department of Computer Science and Technology, University of Cambridge, CB3 0WA Cambridge, U.K. (e-mail: g.gradoni@surrey.ac.uk).

Digital Object Identifier 10.1109/TAP.2026.3662161

and actuators (i.e., electromagnets) is unnecessary. One of the disadvantages of the reconfigurable reflectarray antennas using electromagnets is that multibit (or continuous) tunability is not easily achievable because of the nonlinearity of the magnetostatic force.

On the other hand, the so-called magnetic gear has been studied as a promising mechanical actuation system [33], [34], [35], [36]. The magnetic gear is the counterpart of a mechanical gear and is composed of an array of static magnets instead of gears. Owing to the magnetostatic force between the static magnets, torque can be transmitted easily from one magnetic gear to the other in a contactless manner. The magnetic gear is one kind of direct-drive system, which has been used as an antenna pointing system for a reflector antenna of a satellite communications system [37], [38]. Classical direct-drive systems actuate the reflector antenna using linear motors, which are composed of static magnets and coils. The static magnets are on top of a supporting structure of the reflector antenna, and the reflector antenna moves via Lorentz force in a contactless manner once current is applied to coils, which are installed to bottom of the reflector antenna. As a result, the classical direct-drive system requires a current (or voltage) source to antenna side for driving the coils. On the other hand, the magnetic gear system is usually composed of static magnets, and the current (or voltage) source for driving the coils is unnecessary. Owing to recent advances in static magnets, such as neodymium magnets and 3-D printing technologies, the magnetic gear system can be easily miniaturized and introduced to antenna design.

In this article, a novel reconfigurable antenna using a magnetic gear is proposed. The proposed antenna is composed of a folded monopole element surrounded by floating inverse T-shaped director/reflector elements. The floating inverse T-shaped director/reflector elements are supported by a frame of the upper half of the magnetic gear, and their lower half is behind a ground plane. The magnetic gear is composed of a pair of arrays of small magnets and bearings so that its upper half couples with its lower half via magnetostatic force. The magnetostatic force can penetrate the ground plane, and the upper half of the magnetic gear can rotate in a contactless manner once its lower half rotates mechanically. The advantages of the proposed reconfigurable antenna over conventional ones are as follows.

1) Due to the contactless actuation of an antenna element, a mechanical connection between the antenna element and an actuator is unnecessary. The resultant actuation system is ideally free from friction and abrasion by mechanical contact of gears, and potentially contributes to mechanically maintenance-free actuation system.
2) Spacing between the magnetic gears is constant during actuation, and the resultant magnetostatic force between them is stable. Therefore, magnetic gears do not suffer from the nonlinearity of the magnetostatic force, unlike conventional actuation systems using electromagnets, which tune spacing between the magnets directly. As a result, multibit (or continuous) actuation is easily achievable using the magnetic gear.

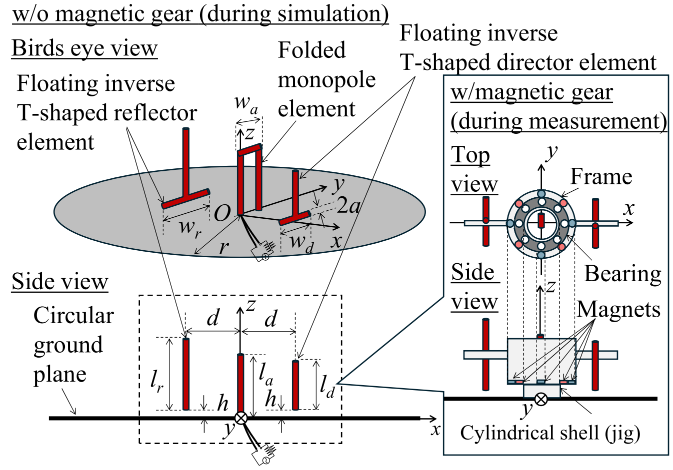

Fig. 1. Geometry of proposed Yagi–Uda monopole antenna.

3) The insertion loss of the actuation system can be kept low. For example, the dielectric loss of the magnetic gear frame becomes small once an infill rate is set to be small during its fabrication using a 3-D printer. Also, the magnetic loss of an array of magnets can be kept low as long as the size of the magnets is smaller than the wavelength under study.

This article is organized as follows. Concept and design of the proposed antenna are demonstrated in Section II. The mechanism of the magnetic gear is described, and fabricated prototype of the proposed antenna is shown in Section III-A. Radiation performance of the proposed antenna is demonstrated experimentally in Section III-B. Section IV concludes this article.

II. Antenna Design and Simulation

A. Concept

The proposed reconfigurable Yagi–Uda monopole antenna is illustrated in Fig. 1. The proposed antenna is composed of a folded monopole element, floating inverse T-shaped reflector/director elements, and a circular ground plane. Owing to the folded monopole element, low radiation resistance of the monopole element can be stepped up, and input impedance of the proposed antenna is expected to be matched to 50 Ω load at an operating frequency band. The reflector/director elements are not connected to the circular ground plane and float to keep tunable directivity by rotating them using a magnetic gear around the folded monopole element. Although the floating reflector/director elements contribute to tunable directivity, the following expected problem must be solved. According to image theory, for a typical Yagi–Uda monopole antenna, it is well-known that the length of the reflector/director monopole elements vertically connected to an infinite ground plane should be half of their equivalent dipole elements, simply. However, for the proposed antenna, the reflector/director elements are vertically floating on the infinite ground plane, and their length is expected to be longer than that of the typical Yagi–Uda monopole element because of the spacing (i.e., electrical discontinuity) between the elements and the

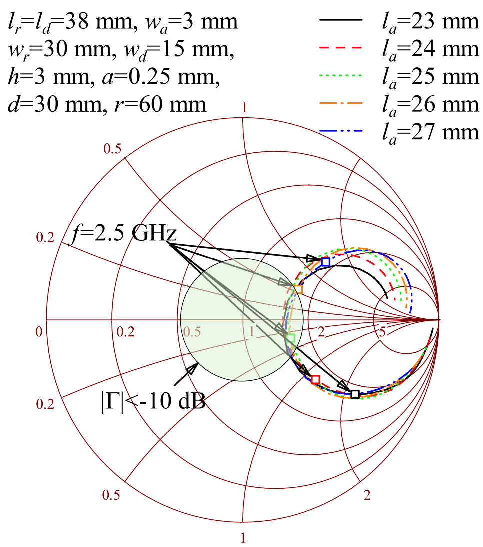

Fig. 2. Input impedance and reflection coefficient of the proposed antenna with different length l_a of folded monopole element.

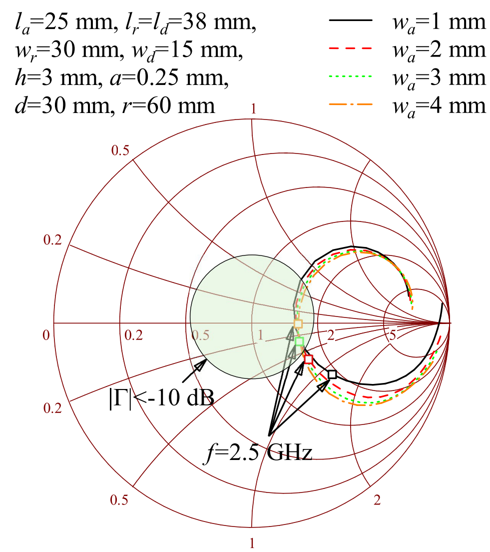

Fig. 3. Input impedance and reflection coefficient of the proposed antenna with different width w_a of folded monopole element.

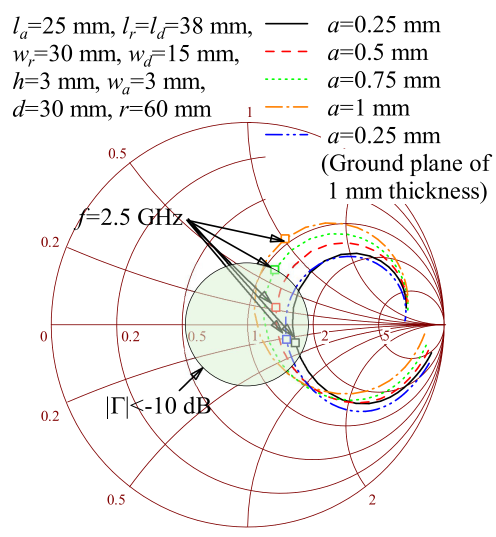

Fig. 4. Input impedance and reflection coefficient of the proposed antenna with different radius a of folded monopole element.

ground plane. The long reflector/director elements result in a high profile of the proposed antenna, and their height should be reduced as much as possible. In order to solve this problem, inverse T-shaped elements are introduced to the reflector/director elements in this article. Owing to T-shaped elements, the length of the reflector/director elements is kept enough without increasing their height. Unintentional radiation of cross-polarization components from the horizontal branch of the T-shaped elements is expected to be suppressed once the T-shaped elements are inversely arranged and their horizontal branch is close to the ground plane.

B. Numerical Simulation

This article focuses on demonstrating the performance of reconfigurable antennas using a magnetic gear. Therefore, the operating frequency of the proposed antenna is set to the 2.5-GHz band because of ease of fabrication. Numerical simulation of the proposed antenna was performed using the method of moments (MoM) by the commercial simulator software FEKO. During the numerical simulation, a magnetic gear, i.e., an array of magnets, bearing, their dielectric supporting structure, including supporting arms for the floating director/reflector elements, was ignored because size of the magnets is negligibly small in comparison with wavelength @f = 2.5 GHz band and effective relative permittivity of the dielectric supporting structure is expected to be almost unity as mentioned later.

Figs. 2 and 3 are Smith charts demonstrating input impedance and reflection coefficient of the proposed antenna with different length l_a and width w_a of the folded monopole element, respectively. Owing to the folded element, the input resistance of the proposed antenna steps up and approximately keeps 70 ~ 80 Ω at the 2.5-GHz band, which is equivalent to that of the half-wavelength dipole antenna. On the other hand, it is found that the input reactance of the proposed antenna shifts from capacitive to inductive at higher frequency bands as l_a and w_a decrease. As a result, the resonance frequency of the proposed antenna gradually shifts to a higher frequency band as l_a and w_a decrease, and vice versa. However, it is found that the resonance frequency of the proposed antenna becomes almost the same once the total length of the folded monopole element (= $2l_a + w_a$) is the same. For example, resonance frequency of the proposed antenna corresponding to $2l_a + w_a$ = 51 mm is 2.6 GHz for (l_a, w_a) = (24 mm, 3 mm), (see red dashed line in Fig. 2) and also (l_a, w_a) = (25 mm, 1 mm), (see solid black line in Fig. 3). Therefore, it can be concluded that the total length of the folded element should be designed so that impedance matching of the proposed antenna is kept at a specific resonance frequency.

Fig. 4 is a Smith chart demonstrating input impedance and reflection coefficient of the proposed antenna with different radius a of the folded monopole element. It is found that

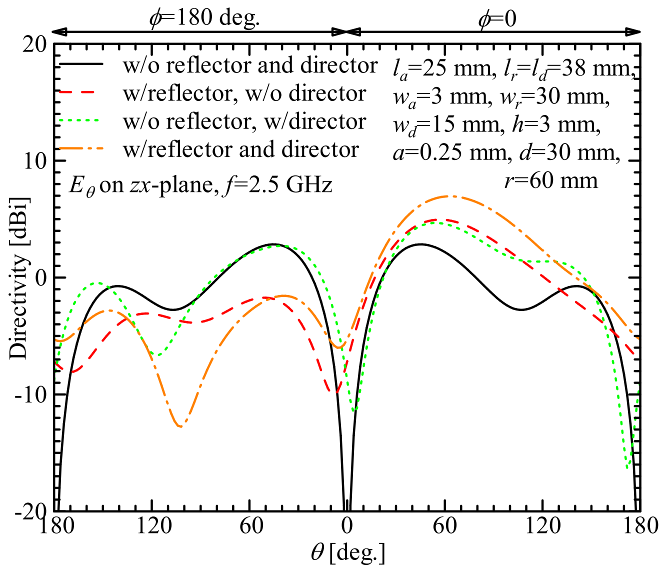

Fig. 5. Effect of director/reflector elements on directivity of the proposed antenna. E_θ on zx-plane. Level of cross polarization components is below −20 dBi and out of range of this graph.

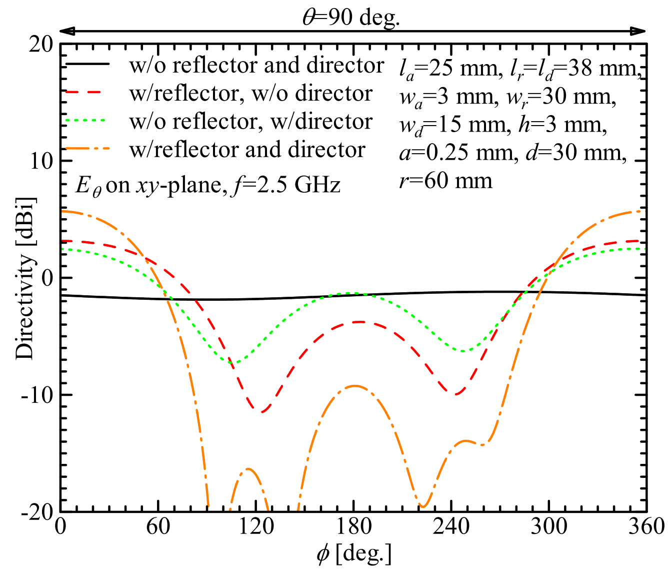

Fig. 6. Effect of director/reflector elements on directivity of the proposed antenna. E_θ on xy-plane. Level of cross polarization components is below −20 dBi and out of range of this graph.

the input resistance of the folded monopole element gradually increases as its radius a decreases at the 2.5-GHz band. On the other hand, in a similar manner to l_a and w_a, the input reactance of the proposed antenna shifts from capacitive to inductive at higher frequency bands as a decreases. As a result, it is found that the resonance frequency of the proposed antenna gradually shifts higher frequency band as a decreases. It is well-known that the so-called impedance step-up ratio (or transformation ratio) is a function of w_a and a [39], [40]. The shift of resonance frequency by tuning a (and also w_a) stems from the different step-up ratio. At the end of the discussion here, supplementary comments on the effect of the finite thickness of the ground plane are described. As described later, a finite thickness of the ground plane can result in a slight shift of the resonance frequency on the fabricated prototype. For example, the results of numerical simulation (blue dash-dot-dotted line in Fig. 4) demonstrate that a 1 mm thickness of the ground plane results in a slight shift of the resonance frequency to the lower frequency band.

Owing to the numerical simulation results, it can be concluded that the proposed antenna can be designed so that its impedance matching is kept at a specific resonance frequency by tuning l_a, w_a, and a. Finally, $l_a = 25$ mm, $w_a = 3$ mm, and $a = 0.25$ mm are chosen as the optimum dimensions of the folded monopole element here from the viewpoints of impedance matching and ease of fabrication. Fractional bandwidth of the proposed antenna with these dimensions, where its reflection coefficient is below −10 dB, is 4%.

Fig. 5 is directivity of the proposed antenna on zx-plane at $f = 2.5$ GHz. Here, the length and width of the floating inverse T-shaped director/reflector elements l_d, w_d, l_r, and w_r are optimized in advance of the numerical simulation so that the directivity of the proposed antenna is maximized at $f = 2.5$ GHz. Finally, $l_d = 38$ mm, $w_d = 15$ mm, $l_r = 38$ mm, and $w_r = 30$ mm are chosen as the optimum dimensions of the floating inverse T-shaped director/reflector elements here. It is noteworthy that the total length of the floating inverse T-shaped director element ($= l_d + w_d$) is 53 mm and is slightly shorter than 0.5 λ (= 60 mm) @ $f = 2.5$ GHz, whereas that of the floating inverse T-shaped reflector element ($= l_r + w_r$) is 68 mm and is slightly longer that 0.5 λ @ $f = 2.5$ GHz. As mentioned earlier, this implies that the total length of the floating inverse T-shaped director/reflector elements should be comparable to that of director/reflector dipole elements of typical Yagi–Uda dipole elements (not monopole elements) for maximizing the directivity. According to Fig. 5, it is found that directivity on the zx-plane is enhanced owing to the floating inverse T-shaped director/reflector elements. The maximum directivity is 7 dBi at $\theta = 62°$, and the main beam is tilted from $\theta = 90°$ because of the effect of a finite ground plane. Level of cross polarization components on zx-plane is below −20 dBi and out of range of Fig. 5.

Fig. 6 is directivity of the proposed antenna on xy-plane at $f = 2.5$ GHz. It is clearly found that radiation to the back side of the proposed antenna ($\phi = 180°$) is suppressed by the floating T-shaped reflector element, whereas that to the front side of the proposed antenna ($\phi = 0$) is enhanced by the floating T-shaped director element.

For specific applications such as base station antennas, it is important to clarify the effect of the size of the ground plane on the directivity of the proposed antenna. Fig. 7 shows the directivity of the proposed antenna with different sizes of the ground plane, i.e., $r = 60, 90, 120$ mm and $r = \infty$. It is found that the directivity of the proposed antenna increases as the size of the ground plane increases. Main beam direction of the proposed antenna with finite r is tilted, whereas that with infinite r is endfire direction ($\theta = 90°$).

According to the numerical simulation results here, it can be concluded that the proposed antenna working at $f = 2.5$ GHz was designed successfully.

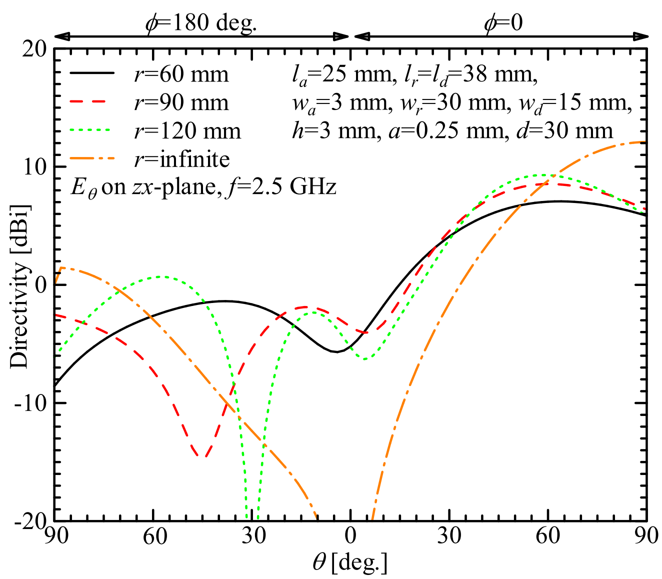

Fig. 7. Effect of the size of the ground plane on directivity of the proposed antenna. E_θ on zx-plane.

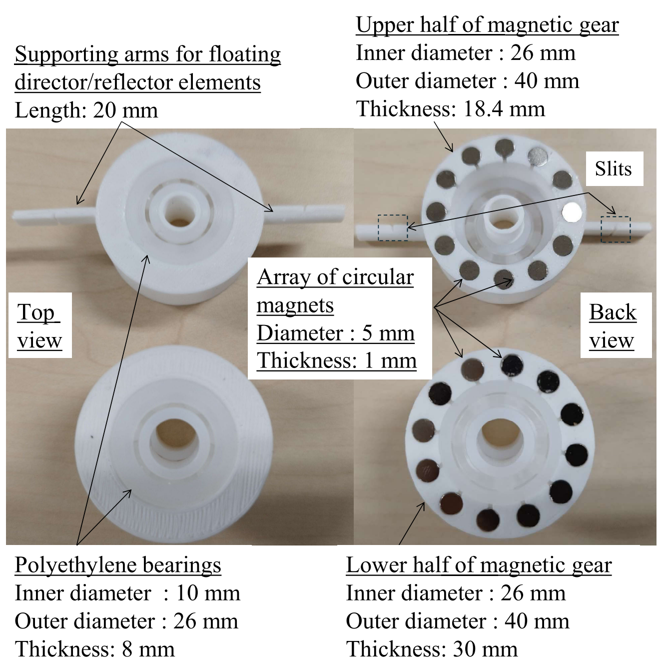

Fig. 8. Fabricated prototype of magnetic gear.

III. Fabrication and Measurement

A. Magnetic Gear and Antenna

A fabricated prototype of a magnetic gear is shown in Fig. 8. The magnetic gear is composed of a pair of arrays of circular magnets, polyethylene bearings, and frames made of polylactic acid (PLA) whose relative permittivity is approximately 2.7 [41], [42].

The magnetic gear frames are separated into the upper half and the lower half. The upper half of the magnetic gear frame has two supporting arms with slits for holding the floating inverse T-shaped director/reflector elements. The polyethylene bearings were set to the center of the upper/lower half of the magnetic gear frames. Both magnetic gear frames were fabricated by a 3-D printer, Flashforge Guider 2s. During fabrication of the frames, the infill rate was 15%, and the resultant effective relative permittivity of the frames is approximately estimated as $\varepsilon_e^r = 1.26$ [41], [42].

The magnets are circularly arranged on the back side of the magnetic gear frames so that the north pole and south pole of the magnets are directed to the same side one after the other. The upper half and the lower half of the magnetic gear are arranged so that the north pole of the magnets on their back side faces the south pole of the magnets on the other half, and vice versa. Although the magnetic gears are separated by the circular ground plane, as shown in Fig. 9(a) and (b), they are magnetostatically coupled via the magnetostatic force penetrating it. Once the bottom half of the magnetic gear is rotated by an actuator, its torque is transmitted to the upper half of the magnetic gear via magnetostatic force in a contactless manner. Therefore, a mechanical connection between an antenna element and an actuator is unnecessary for the proposed antenna. Unlike conventional 1-bit actuation systems using electromagnets [30], the magnetic gear is free from the nonlinearity of the magnetostatic force because the spacing between the upper half and lower half of the magnetic gears is constant during actuation, and the resultant magnetostatic force between them is stable. As a result, the antenna element (i.e., floating inverse T-shaped director/reflector elements, here) is continuously tunable using the magnetic gear.

The magnetic gear is automatically controlled by a laptop computer using Arduino UNO R3 and a ULN2003 driver board, as shown in Fig. 9(b). The ULN2003 driver board is connected to a unipolar stepping motor 28BYJ-48. The proposed antenna is mechanically stable, and no vibration is observed as the magnetic gear rotates. Rotation speed of the stepping motor 28BYJ-48 is 15 r/min, approximately. High-speed rotation of the magnetic gear over 3000 r/min is achievable once the stepping motor is replaced with the high performance one [43]. Therefore, it is expected that the scanning speed of the magnetic gear is potentially in the ms order, whereas that of the electronic counterparts is in μs order [44]. It should be noteworthy that high-speed rotation of the magnetic gear may result in unintentional problems such as eddy current loss and heating, which are negligible for the fabricated prototype. A magnetic shield or another remedy may be necessary for these problems, but they are beyond the scope of this article. Also, the proposed antenna is free from magnetization and hysterisis effects because it is composed of nonmagnetic material (except for static magnets).

Fig. 9(c) shows assembly of the proposed antenna. First, a folded monopole antenna is soldered on the circular ground plane. Next, the polyethylene bearing, which is supported by a cylindrical shell pinched by plastic screws, is loaded with the folded monopole antenna so that the folded monopole antenna is inside. Finally, the upper half of the magnetic gear with the inverse T-shaped director/reflector elements is loaded with the polyethylene bearing.

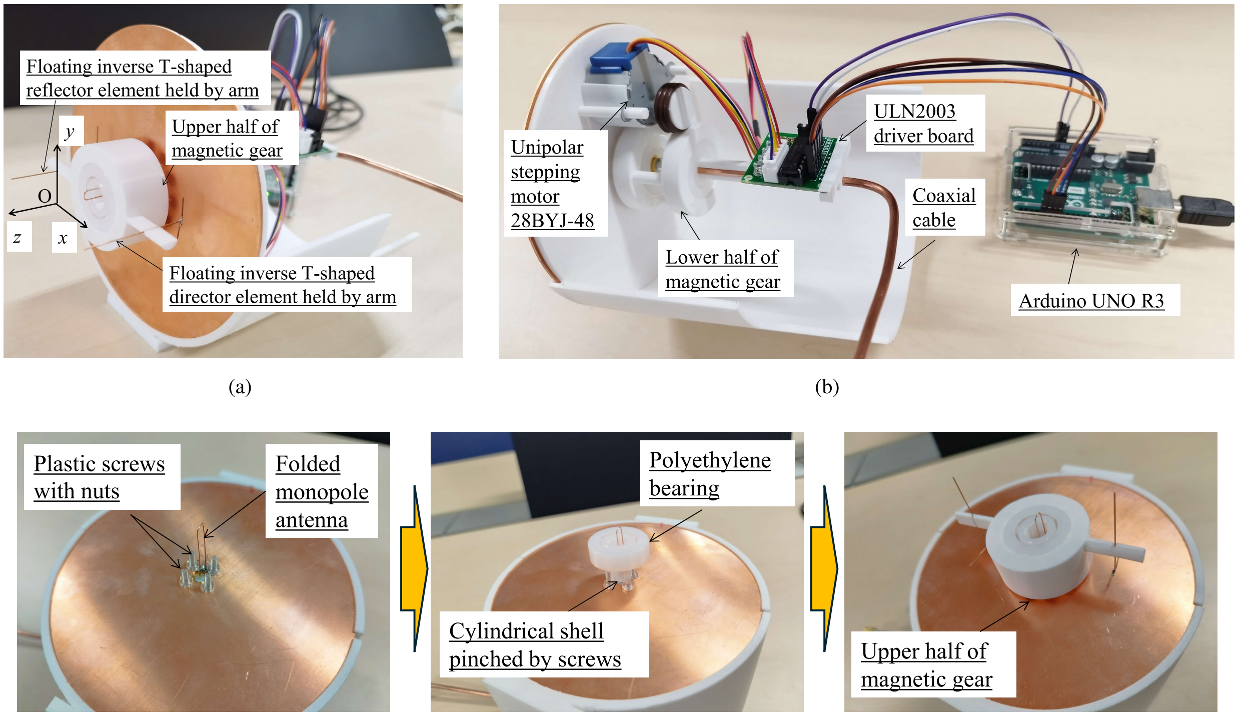

(a) (b)

(c)

Fig. 9. Fabricated prototype of proposed antenna. (a) Upper side. (b) Lower side. (c) Assembly of the upper side.

B. Measurement

Here, the measured radiation performance of the proposed antenna is shown. Input impedances and reflection coefficients were measured using a vector network analyzer, Anritsu MS46524B. Gain of the proposed antenna was measured using a three-antenna method inside our radio anechoic chamber. In addition to the proposed antenna, a double ridged horn antenna Schwarzbeck BBHA 9120D and a log periodic dipole array antenna Electro-Metrics EM-6952 were used. During measurement of the gain, a CW signal was delivered to a transmitting antenna by a signal generator Rohde & Schwarz SMR20. A receiving antenna on a turntable is connected to a spectrum analyzer Keysight N9324C via a preamplifier Hewlett Packard 8449B.

Fig. 10 shows the measured input impedance and reflection coefficient of the proposed antenna. In order to clarify effect of the magnetic gear on input performance of the proposed antenna, measured input impedance and reflection coefficient of following antennas are shown in Fig. 10. The folded monopole antenna, the folded monopole antenna with magnetic gear frame (without array of circular magnets and inverse T-shaped director/reflector elements), the folded monopole antenna with magnetic gear (with array of circular magnets and without inverse T-shaped director/reflector elements). Fig. 10 shows that measured input resistance (black solid line) agrees well with that of numerical simulation (red dashed line), whereas measured input reactance shifts from that of numerical simulation. As a result of the shift of input reactance, the resonance frequency of the proposed antenna shifts from 2.5 to 2.35 GHz for the fabricated prototype. The shift of input reactance stems from the effect of the magnetic gear frame, including the polyethylene bearing, because the shift is observed between the measured input reactance of the folded monopole element (green dotted line) and that with the magnetic gear frame (orange dash-dotted line). On the other hand, the effect of the array of circular magnets is negligible on the input performance of the proposed antenna because the

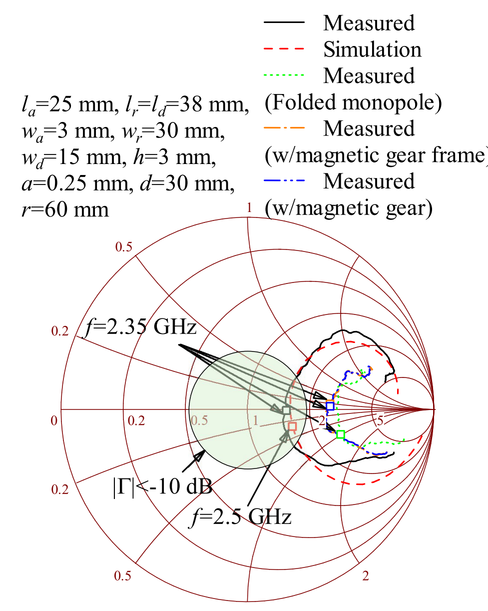

Fig. 10. Measured input impedance and reflection coefficient of the proposed antenna.

measured input impedance of the folded monopole element with the magnetic gear frame (orange dash-dotted line) agrees well with that of the magnetic gear (blue dash-double-dotted line). Although a shift of the resonance frequency is found, it can be concluded that the fabricated antenna works. Fractional bandwidth of the proposed antenna, where its measured reflection coefficient is below −10 dB, is 4.5%. According to the measured results, it is clarified that the effect of the magnetic gear on the input performance of the proposed antenna is a shift of the resonance frequency.

To elaborate on the effect of the magnetic gear frame on the resonance frequency of the proposed antenna, the effect of the magnetic gear with different infill rates on the resonance frequency of the proposed antenna is shown in Fig. 11. According to Fig. 11, following two insights are found.

1) The resonance frequency of the proposed antenna is almost constant as a function of infill rate and is the same as that with the polyethylene bearing. Therefore, it is found that the shift of the resonance frequency of the proposed antenna mainly comes from the polyethylene bearing, which is in the vicinity of the folded monopole element.
2) The resonance frequency is 2.35 GHz for the measured reflection coefficients, whereas it is 2.4 GHz for the simulated reflection coefficients. Discrepancy between the measured and simulated resonance frequency is expected to come from the difference between the fabricated prototype and the simulation model, such as fabrication error.

To find the effect of fabrication error on the resonance frequency of the proposed antenna, the simulated resonance frequency f_r of the proposed antenna with different lengths l_a and widths w_a of the folded monopole element is shown in Fig. 12. According to Fig. 12, it is found that a 1-mm error of l_a results in 0.05 ∼ 0.01 GHz shift of resonance frequency, which is equivalent to the discrepancy between the measured and simulated resonance frequency. Although l_a of the fabricated prototype is l_a = 25 mm and is the same as the simulation model, the finite thickness (=1 mm) of the ground plane, which is zero during numerical simulation, contributes to extending l_a of the fabrication prototype, effectively. Therefore, it can be concluded that the discrepancy between the measured and simulated resonance frequency comes from the finite thickness of the ground plane for the fabricated prototype.

Fig. 13 is the measured antenna gain pattern of the proposed antenna. Here, it should be noted that the antenna gain pattern was measured at 2.35 GHz, not 2.5 GHz, because the shift of resonance frequency from 2.5 to 2.35 GHz was observed on the measured input impedance. It is found that the measured antenna gain pattern agrees well with that of the simulated one. Measured antenna gain and 3-dB beamwidth are 6 dBi and 59°, whereas simulated ones are 6.2 dBi and 76°. Measured cross polarization level is below −13.4 dBi, and its degradation from the simulated one (below −20 dBi) stems from cables or jigs during measurement. As discussed in the following paragraph, the 0.2 dB difference between simulated and measured antenna gain mainly stems from the magnetic gear itself.

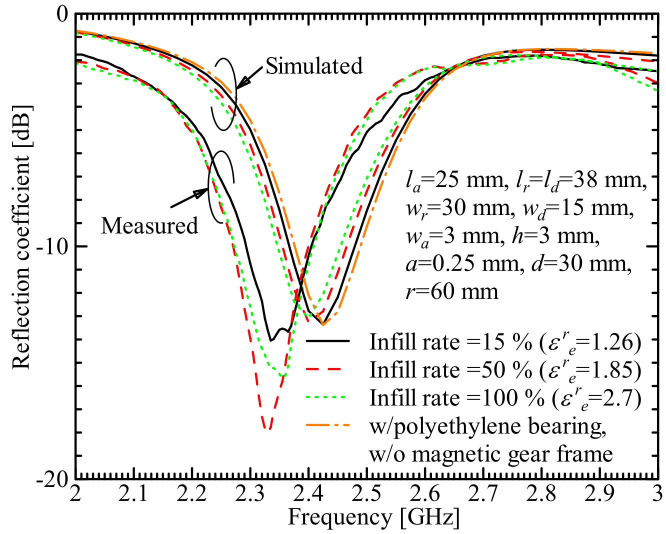

Fig. 11. Reflection coefficient of the proposed antenna with different infill rates of the magnetic gear frame. During numerical simulation, polyethylene bearing (whose relative permittivity is 2.4) and magnetic gear frame (ε_e^r = 1.26, 1.85, 2.7) are modeled as a free-standing, uniform dielectric cylindrical shell. An array of magnets is absent from the simulation model.

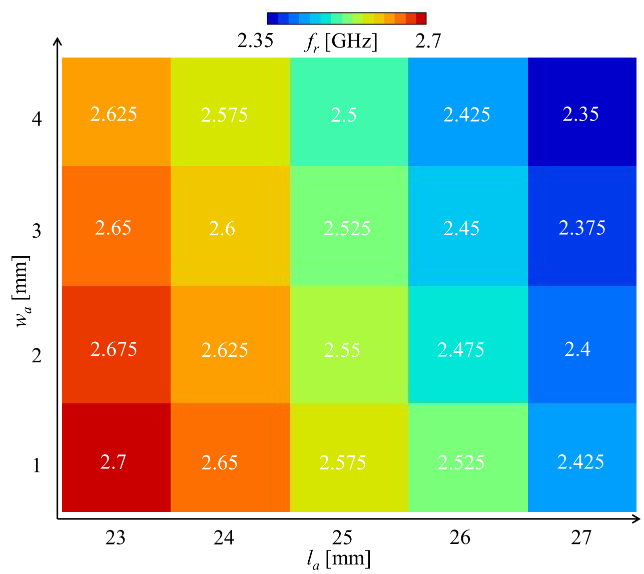

Fig. 12. Simulated resonance frequency f_r of the proposed antenna with different length l_a and width w_a of folded monopole element ($l_r = l_d$ = 38 mm, w_r = 30 mm, w_d = 15 mm, h = 3 mm, a = 0.25 mm, d = 30 mm, r = 60 mm). Magnetic gear is absent from the simulation model.

In order to clarify the effect of the magnetic gear on the radiation performance of the proposed antenna, measured antenna gain patterns of the following antennas are shown in Fig. 14. The folded monopole antenna, the folded monopole antenna with magnetic gear frame (without array of circular magnets and inverse T-shaped director/reflector elements), the folded monopole antenna with magnetic gear (with array of circular magnets and without inverse T-shaped director/reflector elements). According to the measured antenna gain patterns, it

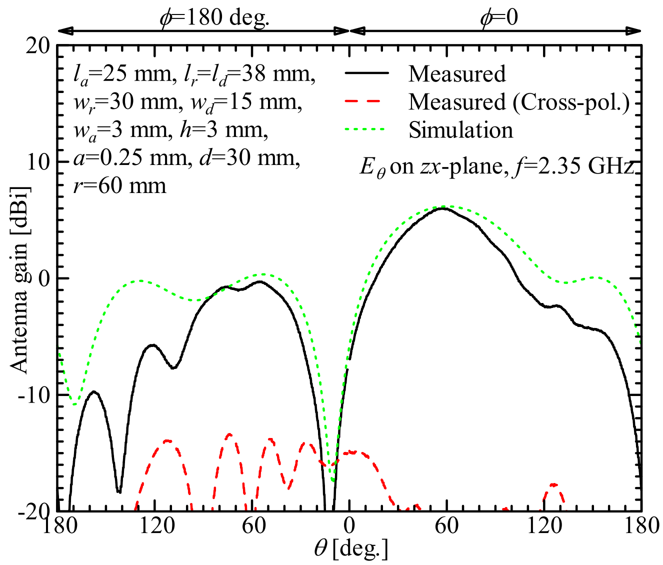

Fig. 13. Measured antenna gain pattern of the proposed antenna. Level of simulated cross polarization components is below −20 dBi and out of range of this graph.

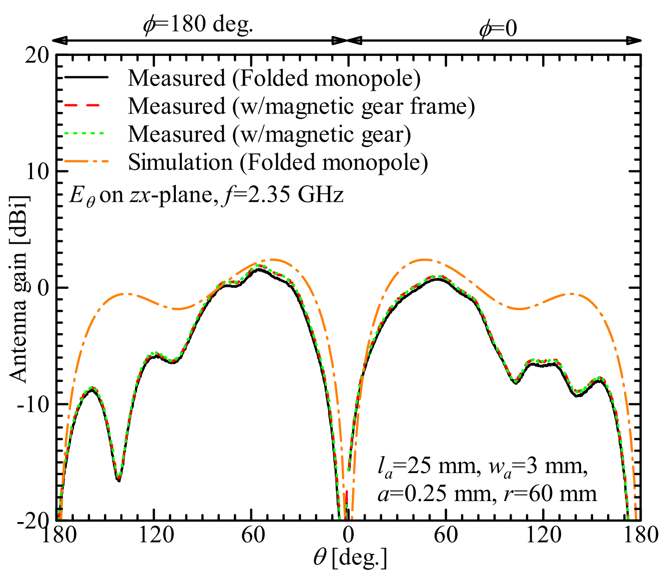

Fig. 14. Measured antenna gain patterns of the folded monopole antenna w/ and w/o magnetic gear (frame).

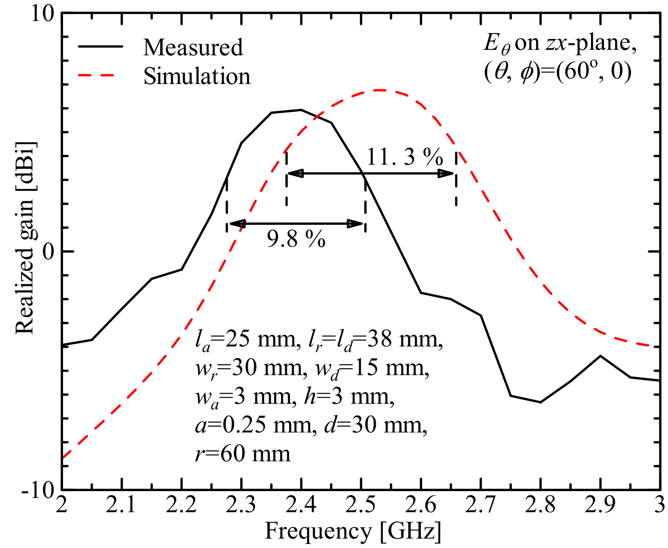

Fig. 15. Measured bandwidth of realized gain of the proposed antenna at its main beam direction.

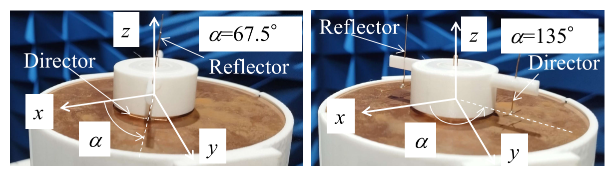

Fig. 16. Rotation angle α of the floating inverse T-shaped director/reflector elements.

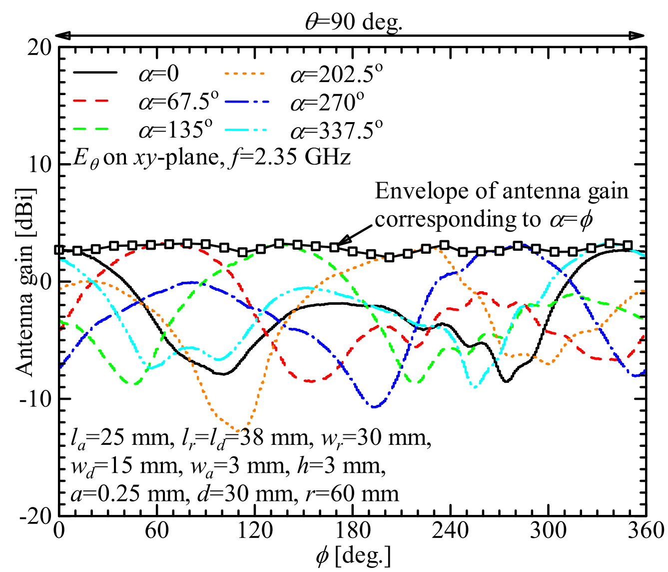

Fig. 17. Measured pattern reconfigurability of the proposed antenna. E_θ on xy-plane.

is found that the effect of the magnetic gear frame and array of circular magnets on the radiation patterns of the folded monopole antenna is quite small. The difference between the measured antenna gain levels is approximately 0.2 dB at their mainbeam direction. Therefore, it can be concluded that the effect of the magnetic gear on the radiation performance of the proposed antenna is at most 0.2 dB and negligible.

Bandwidth of the realized gain of the proposed antenna at its mainbeam direction $(\theta, \phi) = (60^\circ, 0)$ was measured and shown in Fig. 15. Except for the shift of resonance frequency by effect of the magnetic gear and fabrication error, the measured frequency response agrees well with the simulated one. Measured fractional 3-dB bandwidth of the proposed antenna is 9.8%, whereas the simulated one is 11%.

Finally, the rotation angle α of the floating inverse T-shaped director/reflector elements shown in Fig. 16 is reconfigured, and pattern reconfigurability of the proposed antenna is demonstrated. Fig. 17 shows the measured antenna gain of

TABLE I
PERFORMANCE COMPARISON OF PATTERN RECONFIGURABLE YAGI–UDA ANTENNAS

Mechanism	Frequency [GHz]	Size [mm^3]	Gain [dBi]	Fractional bandwidth [%]	Scanning range, Resolution	Insertion loss [dB]
Stretch of liquid metal [45]	2.45	80 × 50 × 84	7.8	3.3	Forward-backward, 1 bit	N/A
Sector beam switching [46]	3	150 × 150 × 32^{†1}	7.5^{†1}	10^{†1}	Full 360° azimuth, 20 deg.^{†2}	N/A
Biasing diodes [47]	2.4	150 × 100 × 0.5	6.2	8.3	Forward-backward, 1 bit	∼ 0.9
Gravity [48]	2.45	126 × 126 × 28	6.8	13	Full 360° azimuth, N/A	N/A
Biasing diodes [49]	2.72	18 × 18 × 15^{†3}	5.4	7.4	Full 360° azimuth, 3 bits	∼ 1.1
Magnetic gear(This work)	2.35	120 × 120 × 41	6	4	Full 360° azimuth, 5 bits	∼ 0.2

^{†1} Performance of single element. ^{†2} Performance of array antennas. ^{†3} Size of ground plane is unavailable and excluded here.

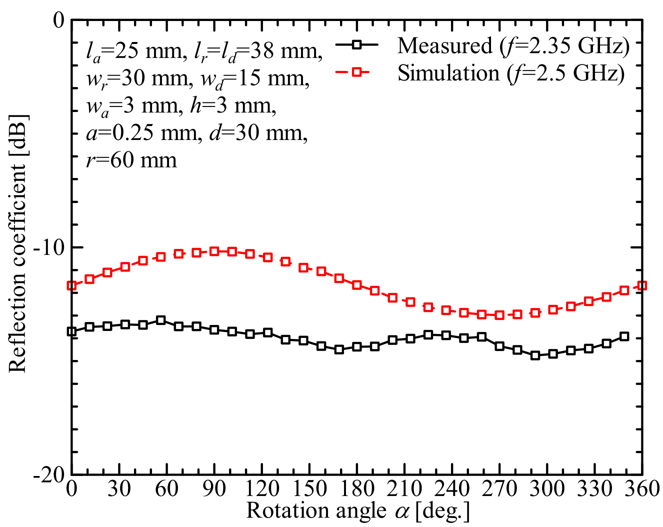

Fig. 18. Measured reflection coefficient of the proposed antenna corresponding to different rotation angle α.

the proposed antenna as a function of the rotation angle α. To demonstrate multibit tunability of the fabricated magnetic gear system, the rotation angle α was tunable with a resolution of five bits, i.e., in increments of 11.25° (= 360°/2^5) during the measurement. Envelope of the antenna gain corresponding to $\alpha = \phi$ is almost uniform, and 5 bits pattern reconfigurability of the proposed antenna has been demonstrated. It should be noted that the measured reflection coefficient was under −13 dB @ 2.35 GHz during rotation, as shown in Fig. 18. According to Figs. 17 and 18, it is found that 5 bits of tunability on the proposed antenna is achievable by the fabricated magnetic gear system.

Finally, performance of the proposed antenna and conventional pattern reconfigurable Yagi–Uda antennas is summarized in Table I. According to Table I, the pros and cons of the proposed antenna over conventional ones are summarized as follows.

1) *Pros:* The finest beam scanning resolution and small insertion loss. The first one stems from linear actuation by the magnetic gear, whereas the second one stems from its contactless actuation. Except for [45] and [48], where the actuation system or its resolution is not specified, it is found that fine beam scanning resolution is only achievable by using multiple elements (i.e., sector beam switching [46]) or multiple diodes (i.e., see [47] and [49]). However, beam switching by multiple elements results in large antenna size (e.g., 374 × 374 × 32 mm^3 is necessary for [46]) and beam scanning by multiple diodes results in large insertion loss (e.g., 14 diodes were used in [47] and four diodes were used in [49]). On the other hand, the beam scanning resolution of the proposed antenna is easily refined by setting a smaller step angle for the magnetic gear without increasing its size and loss. This point is also a clear advantage of the proposed antenna over previous works. It should be noted that the main beam direction of an antenna in [48] is automatically specified by gravity. Therefore, beam scanning to an arbitrary direction in the azimuth plane, which is achievable by the proposed antenna, is not possible for the antenna in [48].
2) *Cons:* Relatively narrow fractional bandwidth and high profile, particularly in comparison with [48]. The former one comes from a folded and thin wire ($2a$ = 0.5 mm) monopole element, whereas Li et al. [48] used an unfolded and thick wire ($2a$ = 3.5 mm) monopole element. The latter one comes from relatively high-profile floating dipole director/reflector elements, whereas Li et al. [48] used monopole director/reflector elements, which have half the length of the dipole counterparts. The fractional bandwidth of the proposed antenna can be enhanced by introducing a wideband element, such as a bowtie element, to the director/reflector elements [50]. Another possible remedy for enhancing the fractional bandwidth of the proposed antenna is to introduce a relatively wide or thick monopole element instead of a narrowband folded monopole antenna [51], [52]. Low-profile design may be achievable by introducing parasitic or meander line elements [53], [54]. Finally, it should be noted that the relatively low gain (6 dBi @ 2.35 GHz) of the proposed antenna, rather than that of [48] (6.8 dBi @ 2.45 GHz), is due to the differences in the operating frequency. It has been confirmed that the simulated gain of the proposed antenna is 6.9 dBi @ 2.45 GHz, although its graph is not shown here for brevity.
3) *Applications:* Transmitting antenna for wireless power transfer or base station antenna for wireless communication. According to the pros and cons shown here, narrowband beam scanning to movable targets is one of the best applications of the proposed antenna. Therefore, the transmitting antenna for wireless power

transfer is a promising application of the proposed antenna. Once the bandwidth of the proposed antenna is enhanced in the future, a base station antenna for wireless communication is also a possible application.

IV. Conclusion

In this article, a novel mechanically reconfigurable Yagi–Uda monopole antenna using a magnetic gear has been proposed. The proposed antenna is composed of a folded monopole antenna and floating inverse T-shaped director/reflector elements. The magnetic gear is composed of an array of circular magnets, a magnetic gear frame made of PLA, and a polyethylene bearing. Owing to magnetostatic coupling between the magnetic gears, the floating inverse T-shaped director/reflector elements held by a magnetic gear frame rotate in a contactless manner. Radiation performance and reconfigurability of the proposed antenna have been demonstrated numerically and experimentally.

An actuation system using a magnetic gear has a couple of advantages over conventional reconfigurable antennas. The first one is a contactless actuation system, which is free from friction and abrasion, potentially leading to mechanically maintenance-free actuation system. The second one is that the actuation system using the magnetic gear is free from the nonlinearity of magnetostatic force that makes the conventional actuation system using electromagnets unstable. The third one is that low insertion loss is achievable once a low infill rate magnetic gear frame and small magnets in comparison with the wavelength under study are used.

Miniaturization of the magnetic gear system, which is applicable for antennas for the high-frequency band, is a future work. According to recent advancement of 3-D printing technologies, the average error in fabrication using a 3-D printer can be reduced to 0.1 ∼ 0.15 mm approximately [55]. Average error of 0.1 ∼ 0.15 mm is comparable to 1/100 wavelength of 20 ∼ 30 GHz band, and scalability of the proposed antenna to high-frequency band, such as the millimeter waveband, is promising.

Acknowledgment

Discussions with the members of the Cooperative Research Project Program of the Research Institute of Electrical Communication, Tohoku University, were helpful for this work.

References

[1] R. Harrington, “Reactively controlled directive arrays,” *IEEE Trans. Antennas Propag.*, vol. AP-26, no. 3, pp. 390–395, May 1978.

[2] R. Dinger, “Reactively steered adaptive array using microstrip patch elements at 4 GHz,” *IEEE Trans. Antennas Propag.*, vol. AP-32, no. 8, pp. 848–856, Aug. 1984.

[3] J. Cheng, Y. Kamiya, and T. Ohira, “Adaptive beamforming of ESPAR antenna based on steepest gradient algorithm,” *IEICE Trans. Commun.*, vol. 84, no. 7, pp. 1790–1800, Jul. 2001.

[4] B. Shishkov, J. Cheng, and T. Ohira, “Adaptive beamforming of ESPAR antenna–unconventional approach,” *IEICE Trans. Electron.*, vol. 85, no. 3, pp. 452–457, Mar. 2002.

[5] B. Shishkov, J. Cheng, and T. Ohira, “Adaptive control algorithm of ESPAR antenna based on stochastic approximation theory,” *IEICE Trans. Commun.*, vol. 85, no. 4, pp. 802–811, Apr. 2002.

[6] Q. Han, K. Inagaki, K. Iigusa, R. Schlub, and T. Ohira, “Reactive-field anechoic box for ESPAR antenna measurement,” *IEICE Trans. Electron.*, vol. 85, no. 7, pp. 1451–1459, Jul. 2002.

[7] Q. Han, K. Inagaki, K. Iigusa, R. Schlub, T. Ohira, and M. Akamine, “Harmonic distortion suppression technique for varactor-loaded parasitic radiator antennas,” *IEICE Trans. Electron.*, vol. 85- no. 12, pp. 2015–2021, Dec. 2002.

[8] K. Ito, A. Akiyama, and M. Ando, “Bandwidth of electronically steerable parasitic array radiator antennas in single beam scanning,” *IEICE Trans. Commun.*, vol. 86, no. 9, pp. 2844–2847, Sep. 2003.

[9] R. Schlub, J. Lu, and T. Ohira, “Seven-element ground skirt monopole ESPAR antenna design from a genetic algorithm and the finite element method,” *IEEE Trans. Antennas Propag.*, vol. 51, no. 11, pp. 3033–3039, Nov. 2003.

[10] J. J. Luther, S. Ebadi, and X. Gong, “A microstrip patch electronically steerable parasitic array radiator (ESPAR) antenna with reactance-tuned coupling and maintained resonance,” *IEEE Trans. Antennas Propag.*, vol. 60, no. 4, pp. 1803–1813, Apr. 2012.

[11] J. J. Luther, S. Ebadi, and X. Gong, “A low-cost 2×2 planar array of three-element microstrip electrically steerable parasitic array radiator (ESPAR) subcells,” *IEEE Trans. Microw. Theory Techn.*, vol. 62, no. 10, pp. 2325–2336, Oct. 2014.

[12] W. Ouyang and X. Gong, “An electronically steerable parasitic array radiator (ESPAR) using cavity-backed slot antennas,” *IEEE Antennas Wireless Propag. Lett.*, vol. 18, no. 4, pp. 757–761, Apr. 2019.

[13] W. Ouyang and X. Gong, “A 20-element cavity-backed slot electronically steerable parasitic array radiator (ESPAR) with 2-D beamsteering and minimized beam squint,” *IEEE Antennas Wireless Propag. Lett.*, vol. 19, no. 8, pp. 1420–1424, Aug. 2020.

[14] P.-Y. Qin, A. R. Weily, Y. J. Guo, T. S. Bird, and C.-H. Liang, “Frequency reconfigurable quasi-Yagi folded dipole antenna,” *IEEE Trans. Antennas Propag.*, vol. 58, no. 8, pp. 2742–2747, Aug. 2010.

[15] Y. Cai, Y. J. Guo, and P.-Y. Qin, “Frequency switchable printed Yagi–Uda dipole sub-array for base station antennas,” *IEEE Trans. Antennas Propag.*, vol. 60, no. 3, pp. 1639–1642, Mar. 2012.

[16] Y. Cai, Y. J. Guo, and T. S. Bird, “A frequency reconfigurable printed Yagi–Uda dipole antenna for cognitive radio applications,” *IEEE Trans. Antennas Propag.*, vol. 60, no. 6, pp. 2905–2912, Jun. 2012.

[17] P.-Y. Qin, Y. J. Guo, and C. Ding, “A beam switching quasi-Yagi dipole antenna,” *IEEE Trans. Antennas Propag.*, vol. 61, no. 10, pp. 4891–4899, Oct. 2013.

[18] C. Kittiyanpunya and M. Krairiksh, “A four-beam pattern reconfigurable Yagi–Uda antenna,” *IEEE Trans. Antennas Propag.*, vol. 61, no. 12, pp. 6210–6214, Dec. 2013.

[19] C. Kittiyanpunya and M. Krairiksh, “Design of pattern reconfigurable printed Yagi–Uda antenna,” *IEICE Trans. Commun.*, vol. 99, no. 1, pp. 19–26, Jan. 2016.

[20] R. C. Brown, P. Clarricoats, and Z. Hai, “The performance of a prototype reconfigurable mesh reflector for spacecraft antenna applications,” in *Proc. 19th Eur. Microw. Conf.*, Oct. 1989, pp. 874–878.

[21] P. J. B. Clarricoats and H. Zhou, “The design and performance of a reconfigurable mesh reflector antenna,” in *Proc. 7th ICAP (IEE)*, vol. 1, 1991, pp. 322–325.

[22] P. J. B. Clarricoats and H. Zhou, “Design and performance of a reconfigurable mesh reflector antenna. Part 1: Antenna design,” *IEE Proc. H Microw., Antennas Propag.*, vol. 138, no. 6, pp. 485–492, 1991.

[23] G. Washington, H.-S. Yoon, M. Angelino, and W. H. Theunissen, “Design, modeling, and optimization of mechanically reconfigurable aperture antennas,” *IEEE Trans. Antennas Propag.*, vol. 50, no. 5, pp. 628–637, May 2002.

[24] V. F. Fusco, “Mechanical beam scanning reflectarray,” *IEEE Trans. Antennas Propag.*, vol. 53, no. 11, pp. 3842–3844, Nov. 2005.

[25] X. Yang et al., “A broadband high-efficiency reconfigurable reflectarray antenna using mechanically rotational elements,” *IEEE Trans. Antennas Propag.*, vol. 65, no. 8, pp. 3959–3966, Aug. 2017.

[26] X. Yang et al., “A mechanically reconfigurable reflectarray with slotted patches of tunable height,” *IEEE Antennas Wireless Propag. Lett.*, vol. 17, no. 4, pp. 555–558, Apr. 2018.

[27] K. Konno, K. Takeda, and Q. Chen, “Beam scanning capability and suppression of endfire radiation of dipole array antennas coupled to two-wire parallel transmission line,” *IEICE Commun. Exp.*, vol. 4, no. 12, pp. 358–362, 2015.

[28] K. Konno, T. Sekiguchi, H. Sato, and Q. Chen, “Continuous beam scanning performance of dipole array antenna coupled to meander two-wire parallel transmission line,” *IEICE Commun. Exp.*, vol. 6, no. 8, pp. 490–495, 2017.

[29] N. Nakamoto et al., "Radial line planar phased array using electromechanically rotated helical antennas," *IEICE Trans. Commun.*, vol. E106.B, no. 2, pp. 174–183, Feb. 2023.
[30] A. Hu, K. Konno, Q. Chen, and T. Takahashi, "A highly efficient 1-bit reflectarray antenna using electromagnet-controlled elements," *IEEE Trans. Antennas Propag.*, vol. 72, no. 1, pp. 506–517, Jan. 2024.
[31] A. Hu, K. Konno, and Q. Chen, "On the field measurement of a highly efficient reflectarray antenna using electromagnets," in *Proc. IEEE Int. Workshop Antenna Technol. (iWAT)*, Apr. 2024, pp. 140–142.
[32] A. Hu, K. Konno, and Q. Chen, "A novel electromagnet-controlled reflectarray element employing 1-bit height locking system with low power consumption," *IEICE Commun. Exp.*, vol. 13, no. 7, pp. 285–288, Jul. 2024.
[33] D. E. Hesmondhalgh and D. Tipping, "A multielement magnetic gear," *IEE Proc. B (Electr. Power Appl.)*, vol. 127, no. 3, pp. 129–138, 1980.
[34] K. Tsurumoto and S. Kikuchi, "A new magnetic gear using permanent magnet," *IEEE Trans. Magn.*, vol. M-23, no. 5, pp. 3622–3624, Sep. 1987.
[35] M. Fukuoka, K. Nakamura, and O. Ichinokura, "Dynamic analysis of planetary-type magnetic gear based on reluctance network analysis," *IEEE Trans. Magn.*, vol. 47, no. 10, pp. 2414–2417, Oct. 2011.
[36] P. M. Tlali, R-J. Wang, and S. Gerber, "Magnetic gear technologies: A review," in *Proc. Int. Conf. Electr. Mach. (ICEM)*, Sep. 2014, pp. 544–550.
[37] E. Tsukuda, Y. Kawakami, S. Miyake, and S. Ogawa, "On-board antenna pointing mechanism for multi-beam satellite communications systems," *JSME Int. J.*, vol. 30, no. 270, pp. 2011–2017, 1987.
[38] I. Noboru and M. Inoue, "Direct drive system for ALMA antenna," *J. Inst. Electr. Eng. Jpn.*, vol. 130, no. 4, pp. 212–215, 2010.
[39] R. Guertler, "Impedance transformation in folded dipoles," *Proc. IRE*, vol. 38, no. 9, pp. 1042–1047, Sep. 1950.
[40] Y. Mushiake, "An exact step-up impedance-ratio chart of a folded antenna," *Trans. IRE Prof. Group Antennas Propag.*, vol. 2, no. 4, p. 163, Oct. 1954.
[41] S. Zhang, Y. Vardaxoglou, W. Whittow, and R. Mittra, "3D-printed graded index lens for RF applications," in *Proc. Int. Symp. Antennas Propag. (ISAP)*, Oct. 2016, pp. 90–91.
[42] A. Hu, K. Konno, and Q. Chen, "A 2-bit 3-D-printed reflectarray antenna using cylindrical rotation-based phase-tunable elements," *IEEE Trans. Antennas Propag.*, vol. 72, no. 10, pp. 7774–7782, Oct. 2024.
[43] Lin Engineering. *WO-208-13-01-RO Datasheet*. Accessed: Dec. 3, 2025. [Online]. Available: https://lin-docs.s3-us-west-2.amazonaws.com/datasheets/digi-key/hybrid-steppers/WO-208-13-01.pdf
[44] H. Kamoda, T. Iwasaki, J. Tsumochi, T. Kuki, and O. Hashimoto, "60-GHz electronically reconfigurable large reflectarray using single-bit phase shifters," *IEEE Trans. Antennas Propag.*, vol. 59, no. 7, pp. 2524–2531, Jul. 2011.
[45] J. Hao, J. Ren, X. Du, J. H. Mikkelsen, M. Shen, and Y. Z. Yin, "Pattern-reconfigurable Yagi–Uda antenna based on liquid metal," *IEEE Antennas Wireless Propag. Lett.*, vol. 20, no. 4, pp. 587–591, Apr. 2021.
[46] Y. Wen, P.-Y. Qin, G.-M. Wei, and R. W. Ziolkowski, "Circular array of endfire Yagi-uda monopoles with a full 360° azimuthal beam scanning," *IEEE Trans. Antennas Propag.*, vol. 70, no. 7, pp. 6042–6047, Jul. 2022.
[47] J. Lu, H. C. Zhang, P. H. He, M. Wang, and T. J. Cui, "Pattern reconfigurable Yagi antenna based on active corrugated stripline," *IEEE Trans. Antennas Propag.*, vol. 71, no. 1, pp. 1011–1016, Jan. 2023.
[48] L. Li, A. Fu, H. Xiong, J. Han, and W. Wu, "Coaxial line and ground separated beam-steering Yagi–Uda antenna controlled by gravity," *IEEE Antennas Wireless Propag. Lett.*, vol. 22, no. 9, pp. 2100–2104, Sep. 2023.
[49] Y. Liu, Z. Wang, and Y. Dong, "Vertically polarized, pattern-reconfigurable, Yagi–Uda dielectric resonator antenna," *IEEE Antennas Wireless Propag. Lett.*, vol. 24, no. 4, pp. 1018–1022, Apr. 2025.
[50] D. Arceo and C. A. Balanis, "A compact Yagi–Uda antenna with enhanced bandwidth," *IEEE Antennas Wireless Propag. Lett.*, vol. 10, pp. 442–445, 2011.
[51] N. P. Agrawall, G. Kumar, and K. P. Ray, "Wide-band planar monopole antennas," *IEEE Trans. Antennas Propag.*, vol. 46, no. 2, pp. 294–295, Feb. 1998.
[52] K.-L. Wong and C.-H. Wu, "Wide-band omnidirectional square cylindrical metal-plate monopole antenna," *IEEE Trans. Antennas Propag.*, vol. 53, no. 8, pp. 2758–2761, Aug. 2005.
[53] H. Nakano, H. Iwaoka, K. Morishita, and J. Yamauchi, "A wideband low-profile antenna composed of a conducting body of revolution and a shorted parasitic ring," *IEEE Trans. Antennas Propag.*, vol. 56, no. 4, pp. 1187–1192, Apr. 2008.
[54] A. A. Omar and Z. Shen, "A compact and wideband vertically polarized monopole antenna," *IEEE Trans. Antennas Propag.*, vol. 67, no. 1, pp. 626–631, Jan. 2019.
[55] P. Minetola, F. Calignano, and M. Galati, "Comparing geometric tolerance capabilities of additive manufacturing systems for polymers," *Additive Manuf.*, vol. 32, Mar. 2020, Art. no. 101103.

Keisuke Konno (Senior Member, IEEE) received the B.E., M.E., and D.E. degrees from Tohoku University, Sendai, Japan, in 2007, 2009, and 2012, respectively.

From 2015 to 2017, he was a Visiting Scholar with the ElectroScience Laboratory, The Ohio State University, Columbus, OH, USA. Since 2012, he has been with the Department of Communications Engineering, Graduate School of Engineering, Tohoku University, where he is currently an Associate Professor. He received a JSPS Post-Doctral Fellowships for Research Abroad. His research interests include computational electromagnetics, array antennas, reflectarrays, and source reconstruction.

Dr. Konno is a member of IEICE. He received the Encouragement Award for Young Researcher and the Most Frequent Presentations Award in 2010 from the Technical Committee on Antennas and Propagation of Japan, the Young Researchers Award in 2011 from the Institute of Electronics, Information and Communication Engineers (IEICE) of Japan, the IEEE EMC Society Sendai Chapter Student Brush-Up Session and EMC Sendai Seminar Student Best Presentation Award in 2011, the JSPS Washington Director Award in 2016, the MHz Rectenna Award in 2017, the Young Researchers Award for ECEI of Tohoku University in 2018, the Minoru Ishida Award in 2018, the IEEE AP-S Japan Young Engineer Award in 2018, the TOKIN Foundation Research Encouragement Award in 2019, and the IEICE Communications Society Distinguished Contributions Awards in 2019 and 2021.

Satoshi Yoshida (Member, IEEE) received the B.S., M.S., and Ph.D. degrees in electrical and communication engineering from Tohoku University, Sendai, Japan, in 2007, 2009, and 2012, respectively.

From 2012 to 2015, he was an Aerospace Project Research Associate with the Institute of Space and Astronautical Science (ISAS), Japan Aerospace Exploration Agency (JAXA), Sagamihara, Japan. From 2015 to 2023, he was an Assistant Professor with the research field in engineering, science, and engineering area, Research and Education Assembly, Kagoshima University, Kagoshima, Japan. Since 2015, he has been a Lecturer with the Faculty of Advanced Science and Technology, Course of Electronics, Information and Communication Engineering, Ryukoku University, Kyoto, Japan. His main research interests include small antennas, active integrated antennas, millimeter-wave antenna systems for wireless communication, and microwave power transmission systems.

Dr. Yoshida was a recipient of the Best Student Paper Award in GSMM 2009, the TAF Telecommunication Student Award in 2011, the IEICE Young Researcher's Award in 2012, and the IEEE Japan Council AP-S Chapters Young Engineer Award in 2012.

Sho Muroga (Member, IEEE) received the B.S., M.S., and Ph.D. degrees from Tohoku University, Sendai, Japan, in 2007, 2009, and 2012, respectively.

From 2012 to 2015, he was an Assistant Professor at Tohoku University. From 2015 to 2017, he was a Lecturer at the National Institute of Technology, Toyota College, Toyota, Japan. From 2017 to 2021 and from 2021 to 2023, he was a Lecturer and an Associate Professor at Akita University, Akita, Japan. Since 2023, he has been an Associate Professor at Tohoku University. His research interests include microwave magnetics, high-frequency electromagnetic measurements, and electromagnetic compatibility.

Dr. Muroga is a member of IEICE, IEEJ, MSJ, and JIEP. From 2011 to 2012, he was a Research Fellow (DC2) of Japan Society for the Promotion of Science (JSPS).

Nozomi Haga (Member, IEEE) was born in Yamagata, Japan, in January 1985. He received the B.E., M.E., and D.E. degrees from Chiba University, Chiba, Japan, in 2007, 2009, and 2012, respectively.

He is currently an Assistant Professor at Gunma University, Gunma, Japan. His main interests have been electrically small antennas, body-centric wireless communication channels, and wireless power transfer systems.

Dr. Haga received the Institute of Electronics, Information and Communication Engineers (IEICE) Technical Committee on Antennas and Propagation: Young Researcher Award in 2012, the IEICE Technical Committee on Wireless Power Transfer: Young Researcher Award in 2018, and the IEEE Antennas and Propagation Society Japan Young Engineer Award in 2018.

Jerdvisanop Chakarothai (Senior Member, IEEE) was born in Suratthani, Thailand, in 1979. He received the B.E. degree in electrical and electronic engineering from Akita University, Akita, Japan, in 2003, and the M.S. and Ph.D. degrees in electrical and communication engineering from Tohoku University, Sendai, Japan, in 2005 and 2010, respectively.

He is currently a Senior Researcher at the National Institute of Information and Communications Technology, Koganei, Tokyo, Japan. His research areas include computational EM, biomedical communications, and electromagnetic compatibility (EMC).

Dr. Chakarothai is a member of the Institute of Electronics, Information and Communication Engineers (IEICE), the Institute of Electrical Engineers, Japan (IEEJ), and the Applied Computational Electromagnetic Society (ACES). He is an Expert Member of the IEC CISPR Subcommittee A. He received the 2014 Young Scientist Award from the International Scientific Radio Union and the Best Presentation Award from IEEJ and IEICE in 2015 and 2018, respectively. He also received the Ulrich L. Rohde Innovative Conference Paper Award on Antenna Measurements and Application in 2018, the Invited Paper Award from the Electronics Society of the IEICE in 2020, and the Best Paper Award from the International Symposium on Antennas and Propagations (ISAP) in 2021.

Qiang Chen (Senior Member, IEEE) received the B.E. degree from Xidian University, Xi'an, China, in 1986, and the M.E. and D.E. degrees from Tohoku University, Sendai, Japan, in 1991 and 1994, respectively.

He is currently the Chair Professor of the Electromagnetic Engineering Laboratory, Department of Communications Engineering, Faculty of Engineering, Tohoku University. His primary research interests include antennas, microwave and millimeter wave, electromagnetic measurement, and computational electromagnetics.

Dr. Chen is a fellow of IEICE. He received the Best Paper Award and Zenichi Kiyasu Award from the Institute of Electronics, Information and Communication Engineers (IEICE). He served as the Chair for the IEICE Technical Committee on Photonics-Applied Electromagnetic Measurement from 2012 to 2014, the Chair for the IEICE Technical Committee on Wireless Power Transfer from 2016 to 2018, the Chair for the IEEE Antennas and Propagation Society Tokyo Chapter from 2017 to 2018, and the Chair for the IEICE Technical Committee on Antennas and Propagation from 2019 to 2021.

Gabriele Gradoni (Member, IEEE) received the Ph.D. degree in electromagnetics from University Politecnica delle Marche, Ancona, Italy, in 2010.

He was a Visiting Researcher with the Time, Quantum, and Electromagnetics Team, National Physical Laboratory, Teddington, U.K., in 2008. From 2010 to 2013, he was a Research Associate with the Institute for Research in Electronics and Applied Physics, University of Maryland, College Park, MD, USA. From 2013 to 2016, he was a Research Fellow with the School of Mathematical Sciences, University of Nottingham, Nottingham, U.K., where he became a Full Professor of applied mathematics and electromagnetics engineering in 2022. Since May 2023, he has been a Full Professor and the Chair of wireless communications at the 6G Innovation Centre, Institute for Communication Systems, University of Surrey, Guildford, U.K. Since June 2020, he has been an Adjunct Associate Professor with the Department of Electrical and Computer Engineering, University of Illinois at Urbana–Champaign, Champaign, IL, USA. Since 2020, he has been a Royal Society Industry Fellow at British Telecom, London, U.K. Since December 2022, he has been a Visiting Fellow with the Department of Computer Science and Technology, University of Cambridge, Cambridge, U.K. His research interests include probabilistic and asymptotic methods for propagation in complex wave systems, metasurface modeling, quantum/wave chaos, and quantum computational electromagnetics, with applications to electromagnetic compatibility and modern wireless communication systems.

Dr. Gradoni is a member of Italian Electromagnetics Society. He received the URSI Commission B Young Scientist Award in 2010 and 2016, Italian Electromagnetics Society Gaetano Latmiral Prize in 2015, and the Honorable Mention IEEE Transactions on EMC Richard B. Schulz Best Paper Award in 2020. From 2014 to 2021, he was the URSI Commission E Early Career Representative.